

Carrier Localization on Surfaces of Organic Semiconductors Gated with Electrolytes

Yu Xia,¹ Wei Xie,¹ P. Paul Ruden,² and C. Daniel Frisbie¹

¹*Department of Chemical Engineering and Materials Science, University of Minnesota, Minneapolis 55455, USA*

²*Department of Electrical and Computer Engineering, University of Minnesota, Minneapolis 55455, USA*

(Received 21 December 2009; revised manuscript received 16 February 2010; published 13 July 2010)

Organic semiconductor single crystals gated with electrolytes exhibit a pronounced maximum in channel conductance at hole densities $>10^{13}$ cm⁻². The cause is a strong decrease in the hole mobility with increasing charge density, which is explained in terms of a percolation model that incorporates trapping of holes by ions at the semiconductor-electrolyte interface. In the case of rubrene crystals, the peak channel conductance occurs at hole densities near 3×10^{13} cm⁻². The magnitude of the effect will be large for semiconductors with low dielectric constants and narrow bandwidths, and thus is likely to be a general phenomenon in organic semiconductors gated with electrolytes.

DOI: 10.1103/PhysRevLett.105.036802

PACS numbers: 73.25.+i, 73.40.Mr, 73.40.Qv, 73.61.Ph

Recently there has been increased interest in employing liquid or solid electrolytes to induce large carrier densities at the surfaces of semiconductors, complex oxides, and nanowire networks [1–6]. In these experiments, the electrolyte serves as a high capacitance gate dielectric in a so-called electrical double-layer transistor (EDLT). When a gate voltage is applied, ions in the electrolyte move to screen the electric field, thereby establishing ultrathin electrical double layers at the gate-electrolyte and semiconductor-electrolyte interfaces. The double-layer capacitance is on the order of 10 μF/cm², which facilitates carrier accumulations in excess of 10¹⁴ cm⁻² [7]. EDLTs have been employed to induce superconductivity at the surfaces of SrTiO₃ and ZrNCl, [8,9] and there is substantial interest in extending electrolyte gating to other systems, including organic semiconductors, that might exhibit gate-induced superconductivity.

Here we address an important effect that occurs when gating organic semiconductors with electrolytes. We show that EDLTs based on single-crystal organic semiconductors exhibit a pronounced peak in the channel conductance as a function of gate voltage; i.e., they exhibit negative transconductance beyond a certain gate voltage. We attribute this effect to the strong interaction of the electrolyte ions with charge carriers at the semiconductor-electrolyte interface, which leads to localization of some of the charge carriers. We expect that at the high charge densities achievable with electrolytes, the resulting decrease of the effective mobility will be operative in any narrow band, low dielectric constant semiconductor. Hence, the result is of general importance to understanding the transport physics of organic systems gated with electrolytes.

We note that the negative transconductance effect has not been reported for conventional semiconductors gated with electrolytes, but has been observed previously for electrolyte-gated polymer semiconductors [10]. Polymer semiconductors, however, are susceptible to electrochemical doping in which the electrolyte penetrates the polymer [11]. Such devices are therefore best referred to as electro-

chemical transistors and the induced structural disorder in these systems may play a role in creating a conductance maximum versus gate voltage. In contrast, for the single-crystal organic semiconductors described here, electrochemical doping does not occur. Indeed, we and others have shown previously that organic crystal surfaces are not disrupted structurally when gated with ionic liquids [6,12]. Ionic liquid gated organic single-crystal devices are thus appropriately described as EDLTs.

Our work focuses on single crystals of the benchmark organic semiconductor rubrene (C₄₂H₂₈) that exhibit room-temperature field effect hole mobilities >10 cm²/V s [13]. Platelike rubrene single crystals several mm in length and width are grown from the vapor phase with the large faces corresponding to the *a-b* plane of the orthorhombic unit cell. Field effect transistors (FETs) are fabricated by laminating a crystal to a rubber stamp precoated with a gold film to form source, drain, and gate contacts, as shown in Fig. 1(a). In previous experiments, the space between the rubrene crystal and the gate electrode is usually evacuated [13–15]. For such vacuum gap FETs, the field effect mobility increases with decreasing temperature from room temperature to ~ 180 K, with maximum mobilities reaching ~ 20 cm²/V s.

For the experiments described here, the vacuum gap between the gate electrode and the rubrene surface was filled with an ionic liquid, 1-ethyl-3-methylimidazolium bis(trifluoromethylsulfonyl)imide [(EMIM)⁺(TFSI)⁻], to make an EDLT [6,12]. The ionic liquid exhibits a very large ionic conductivity (10⁻³ S/cm), but negligible electronic conductivity [16]. It also exhibits exceptional double-layer capacitances >10 μF/cm², which is our motivation for employing it in an EDLT. Application of a gate voltage results in electrical double-layer formation, Fig. 1(b), and an approximate potential profile as shown in the right panel of Fig. 1(b).

The key experimental observation is shown in Fig. 2(a). With the source grounded and a fixed, low drain bias $V_D = -0.1$ V, sweeping the gate voltage V_G in the negative

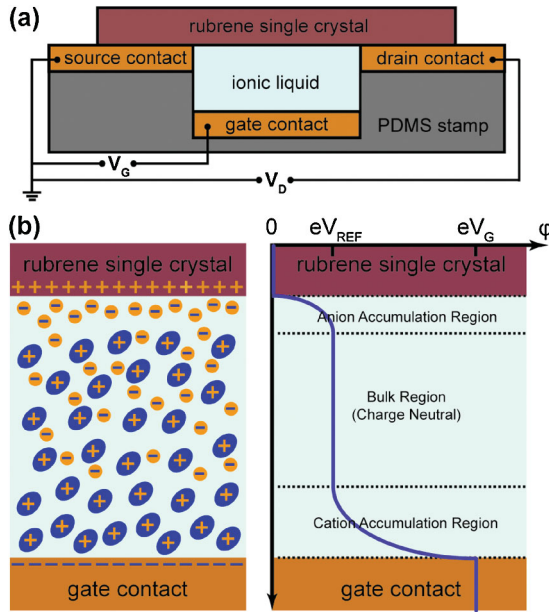


FIG. 1 (color). (a) Scheme showing the cross section of an EDLT based on a rubrene single crystal. (b) Scheme of the channel charge and ion distribution (left) and potential profile (right) of an operating EDLT with bias applied to the gate.

direction results first in an increase in the drain current I_D , and then, beyond -0.45 V, I_D decreases with increasingly negative V_G ; i.e., the I_D - V_G characteristic is peaked and exhibits negative transconductance ($dI_D/dV_G < 0$) for $V_G < -0.45$ V. The I_D - V_G characteristic is reversible and repeatable; multiple sweeps yield identical behavior.

Figure 2(b) displays the induced hole density p as function of V_G , obtained from the measured capacitance-voltage characteristic. Hole density is a monotonically increasing function of V_G and the peak in the I_D - V_G characteristic corresponds to 3×10^{13} cm $^{-2}$ or approximately 0.15 holes per rubrene molecule at the surface of the crystal (the a - b plane of rubrene has a molecular density of 1.9×10^{14} molecules/cm 2).

We estimate the average field effect mobility by dividing the channel conductivity by the carrier concentration at each value of the gate voltage [Fig. 2(c)]. The first observation is that the mobility peaks at $V_G = -0.1$ V and then decreases strongly. Increasing mobility with gate voltage is commonly observed in organic FETs and is usually attributed to trap filling. The important point is that the mobility decreases beyond $V_G = -0.45$ V. The greater than five-fold reduction in effective mobility is the cause of the negative transconductance; over the same V_G range, p only doubles [Fig. 2(b)] so that the product of mobility and p , which is proportional to I_D , decreases.

The second observation is that the maximum mobility is 0.5 cm 2 /V s, a factor of 20 below the value obtained for vacuum gap transistors [13–15]. The ionic liquid apparently reduces the room-temperature mobility [12].

To eliminate the possibility that contacts play a role in the drain current peak, we examined rubrene EDLTs

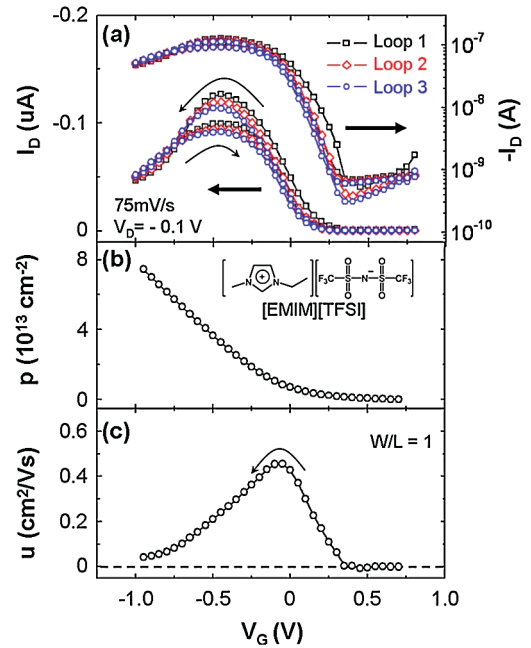


FIG. 2 (color). Electrical characterization of a rubrene single-crystal EDLT. Channel width and length were both 500 μ m. (a) I_D - V_G characteristics for three consecutive V_G sweeps, acquired at the rate of 75 mV/s, at a fixed drain bias $V_D = -0.1$ V. (b) Gate-induced hole density versus V_G , determined from capacitance-voltage measurements. (c) Mobility versus V_G . The inset in (b) shows the molecular structure of the ionic liquid used as the gate dielectric.

with systematically varied channel lengths [Fig. 3(a) and Fig. SP1, (see supplementary information [17])]. Currents scale with channel length as expected. Figure 3(b) displays the channel resistance versus channel length at $V_G = -0.65$ V. The linear relationship verifies that the device is not contact-limited. Figure 3(c) shows both the channel resistance coefficient (i.e., the slope of the resistance versus length plot) and the contact resistance (determined by extrapolation to zero length) as a function of V_G . It is clear that the channel resistance is a nonmonotonic function of V_G and has a minimum at a hole density of $\sim 3 \times 10^{13}$ cm $^{-2}$ ($V_G = -0.6$ V), as anticipated based on Fig. 2(a).

We have also examined the temperature dependence of the I_D - V_G characteristics (Fig. SP2a [17]). The current at any given V_G is thermally activated. Moreover, the activation energy E_A is a decreasing function of V_G (Fig. SP2b). Such trends are normally observed in organic transistors and again are usually attributed to trap filling [18]. The significant point for this discussion is that in the negative transconductance regime ($V_G < -0.45$ V), E_A is not increasing, but instead continues to decrease. Thus, one cannot ascribe the maximum in the I_D - V_G characteristic to an increase in E_A .

To summarize, single-crystal rubrene EDLTs exhibit a peak in the drain current as a function of carrier density, they have a significantly lower effective maximum mobil-

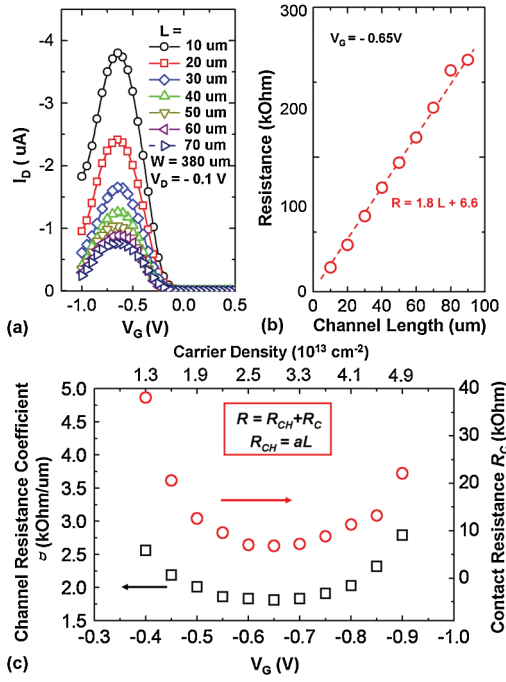


FIG. 3 (color). (a) I_D - V_G characteristics for EDLTs with different channel lengths measured from the same rubrene single crystal. Channel width for all devices was $500 \mu\text{m}$. (b) The resistance-channel length relationship at $V_G = -0.65 \text{ V}$. (c) Summary of channel resistance coefficient [slope of plot in (b)] and contact resistance as a function of gate voltage.

ity than vacuum-gated rubrene FETs, and the transport is activated, with an activation energy that decreases monotonically with increasingly negative V_G .

A key consideration is the role played by discrete ions at the rubrene-electrolyte interface. Rubrene has a low dielectric constant ($k \sim 3$) and a narrow highest occupied molecular orbital (HOMO or valence) bandwidth ($\leq 0.5 \text{ eV}$) [19]. The low dielectric constant and narrow bandwidth can lead to strong interaction of negatively charged anions in the ionic liquid with the positively charged holes at the rubrene surface. With this in mind, we have developed a model based on trapping and percolation transport.

We assume that when the conducting channel is formed, only a thin layer of molecules on the surface of the organic crystal in contact with the ionic liquid hosts the channel charge carriers. There are M such molecules per unit area. Under applied gate bias, N negatively charged ions per unit area will accumulate in essentially the first molecular monolayer of liquid adjacent to the interface. Molecules in the semiconductor are said to be “paired” if they are nearest neighbors to one of the N ions and “unpaired” if they are not. The induced holes in the semiconductor can reside on N paired or $M - N$ unpaired sites. If a hole is located on a paired site it is considered trapped by the Coulomb potential of the neighboring ion of the liquid. The density of holes on semiconductor molecules that are paired with ions is p_p . A hole located on an unpaired

semiconductor molecule is mobile; i.e., it can easily hop to another unpaired molecule. The density of these “free” holes is designated p_f and they are distributed over the $M - N$ unpaired molecules. Charge neutrality requires

$$N = p = p_f + p_p. \quad (1)$$

All densities are sheet densities, and we assume that double occupancy of any semiconductor molecule is suppressed by the holes’ mutual Coulomb repulsion.

In steady state, hopping of holes from unpaired molecules to paired molecules (traps) and the reverse process must balance; therefore,

$$p_f'(N - p_p) = F p_p'(M - N - p_f). \quad (2)$$

Here F is the ratio of the trap emission and capture coefficients. Normalizing Eqs. (1) and (2) with the total density of sites, M , one finds

$$p_f' = \frac{1}{2} \frac{F}{1 - F} \left[\sqrt{1 + \frac{4(1 - F)}{F} N'(1 - N') - 1} \right]. \quad (3)$$

Primes indicate normalized densities. Figure 4 shows the total normalized density of mobile or free holes, p_f' , vs N' for several values of F .

The conductivity of the channel can be thought of in terms of a percolation problem [20]. Of the M sites in the channel, a fraction $f_b = N'$ are blocked (traps). Channel conduction is envisioned as percolation of the free holes through the unblocked sites. The fraction of unblocked sites is $f_{ub} = 1 - f_b$, and conduction is possible if f_{ub} exceeds a threshold f_c . Above this threshold the conductivity increases as a power law with critical exponent t . The unblocked sites are occupied by (free) holes with occupancy $p_f'/(1 - N')$. Combining this with the percolation argument we obtain the conductivity:

$$\sigma \propto \frac{p_f'}{1 - N'} [(1 - N') - f_c]^t. \quad (4)$$

Figure 4 also displays σ vs N' for several different values of F . Here we used $t = 1.1$, which is appropriate for a two-dimensional percolation problem, and we assumed a square lattice, i.e., $f_c = 0.59$ [21]. Note that in the limit of low N' values σ increases because the concentration of free carriers increases. However, at larger N' , the increasing density of blocked sites reduces the conductivity.

As $I_D \propto \sigma$ and $N' \propto (V_T - V_G)$, where V_T is the EDLT threshold voltage, the drain current maximum observed in Figs. 2(a) and 3(a) can be explained by this model. The model is also consistent with the observation of thermally activated transport. Assuming the distribution of holes over the paired and unpaired molecules corresponds to thermal equilibrium, we obtain $F = \exp(-E_{\text{act}}/kT)$ from Eq. (2), where E_{act} is the activation energy that enables hopping from a paired to an unpaired molecule (detrapping). The experimental transport data yield activation energies, E_A , that vary monotonically with V_G : $160 \text{ meV} < E_A < 50 \text{ meV}$ (Fig. SP2). E_A is related to E_{act} ; for small F and

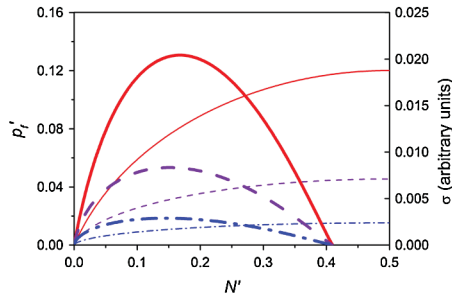


FIG. 4 (color). Model results for the normalized mobile hole density, p_f' (thin lines, left scale), and the conductivity (bold lines, right scale) as a function of the normalized ion density, N' . The solid lines are for $F = 0.1$, the dashed lines for $F = 0.01$, and the dash-dotted lines for $F = 0.001$.

intermediate N' the conductivity of the model described above is approximately proportional to \sqrt{F} , i.e., $E_A \approx E_{\text{act}}/2$. We use this relationship to estimate the relevant range of F : $10^{-5} < F < 10^{-1}$ at room temperature. Furthermore, it seems reasonable that the observed decrease in E_{act} (and thus E_A) with increasing carrier density may be attributable to the increasing overlap of the Coulomb potentials of ions in the liquid with increasing density or it may be due to increasing screening of that interaction.

The model also explains the relatively low effective mobility extracted from the experimental data. In analogy to the procedure for determining the experimental mobility, we define mobility for the model as σ/eN , where e is the elementary charge. Even for the largest F value considered (smallest degree of trapping), the effective mobility determined at the conductivity maximum in Fig. 4 is lower than the bulk mobility by at least a factor of $\sim 1/8$ (peak σ divided by N' for $F = 0.1$). This result is important for organic EDLTs as it suggests that these devices exhibit inherently lower effective mobilities because of ion-induced trapping. The precise dependence of the mobility on the type of ionic liquid [6] may reveal that the mobility lowering effect can be tuned or mitigated.

In summary, single crystals of the benchmark organic semiconductor rubrene exhibit both lower field effect mobilities and a peak in channel conductance when gated with electrolytes. We have explained this effect in terms of ion-induced trapping of carriers at the semiconductor-electrolyte interface in combination with two-dimensional percolative transport. The appearance of the channel conductance peak depends upon the strength of the binding between the carriers and ions at the semiconductor-electrolyte interface. This binding will be favored by high ion densities in the ionic liquid and by low dielectric constants and narrow bandwidths in the semiconductor, and it is thus likely to be general for organic semiconductors gated with electrolytes.

This work was partially supported by the MRSEC Program of the NSF under DMR-0819885. Y. X. acknowledges financial support from the Sundahl program at UMN. PPR and CDF acknowledge stimulating discussions with D.L. Smith and B.I. Shklovskii, and the technical assistance of H.-C. Chang.

- [1] H. Shimotani, H. Asanuma, J. Takeya, and Y. Iwasa, *Appl. Phys. Lett.* **89**, 203 501 (2006).
- [2] M.J. Panzer and C.D. Frisbie, *Adv. Mater.* **20**, 3177 (2008).
- [3] J. Zaumseil, X. Ho, J.R. Guest, G.P. Wiederrecht, and J.A. Rogers, *ACS Nano* **3**, 2225 (2009).
- [4] A.S. Dhoot, C. Israel, X. Moya, N.D. Mathur, and R.H. Friend, *Phys. Rev. Lett.* **102**, 136402 (2009).
- [5] A.S. Dhoot, J.D. Yuen, M. Heeney, I. McCulloch, D. Moses, and A.J. Heeger, *Proc. Natl. Acad. Sci. U.S.A.* **103**, 11 834 (2006).
- [6] S. Ono, K. Miwa, S. Seki, and J. Takeya, *Appl. Phys. Lett.* **94**, 063 301 (2009).
- [7] H. Yuan, H. Shimotani, A. Tsukazaki, A. Ohtomo, M. Kawasaki, Y. Iwasa, *Adv. Funct. Mater.* **19**, 1046 (2009).
- [8] K. Ueno, S. Nakamura, H. Shimotani, A. Ohtomo, N. Kimura, T. Nojima, H. Aoki, Y. Iwasa, and M. Kawasaki, *Nature Mater.* **7**, 855 (2008).
- [9] J. Ye, S. Inoue, K. Kobayashi, Y. Kasahara, H. Yuan, H. Shimotani, and Y. Iwasa, *Nature Mater.* **9**, 125 (2010).
- [10] D. Ofer, R.M. Crooks, and M.S. Wrighton, *J. Am. Chem. Soc.* **112**, 7869 (1990).
- [11] J.D. Yuen, A.S. Dhoot, E.B. Namdas, N.E. Coates, M. Heeney, I. McCulloch, D. Moses, and A.J. Heeger, *J. Am. Chem. Soc.* **129**, 14 367 (2007).
- [12] Y. Xia, J.H. Cho, J. Lee, P.P. Ruden, and C.D. Frisbie, *Adv. Mater.* **21**, 2174 (2009).
- [13] V.C. Sundar, J. Zaumseil, V. Podzorov, E. Menard, R.L. Willett, T. Someya, M.E. Gershenson, and J.A. Rogers, *Science* **303**, 1644 (2004).
- [14] V. Podzorov, E. Menard, A. Borissov, V. Kiryukhin, J.A. Rogers, and M.E. Gershenson, *Phys. Rev. Lett.* **93**, 086602 (2004).
- [15] V. Podzorov, E. Menard, J.A. Rogers, and M.E. Gershenson, *Phys. Rev. Lett.* **95**, 226601 (2005).
- [16] M. Armand, F. Endres, D.R. MacFarlane, H. Ohno, and B. Scrosati, *Nature Mater.* **8**, 621 (2009).
- [17] See supplementary material at <http://link.aps.org/supplemental/10.1103/PhysRevLett.105.036802> for resistance versus channel length and temperature dependence.
- [18] W.L. Kalb, K. Mattenberger, and B. Batlogg, *Phys. Rev. B* **78**, 035334 (2008).
- [19] D.A. da Silva Filho, E. -G. Kim, and J.-L. Bredas, *Adv. Mater.* **17**, 1072 (2005).
- [20] R. Zallen, *The Physics of Amorphous Solids* (John Wiley, New York, 1983).
- [21] B.I. Shklovskii and A.L. Efros, *Electronic Properties of Doped Semiconductors* (Springer-Verlag, Berlin, 1984), and references therein.